13th World Conference on Earthquake Engineering
Vancouver, B.C., Canada
August 1-6, 2004
Paper No. 138

EFFECTIVENESS OF SUPPLEMENTARY DAMPERS FOR ISOLATED BRIDGES UNDER STRONG NEAR-FIELD GROUND MOTIONS

T. Y. LEE [1] and K. KAWASHIMA [2]

SUMMARY

Seismic isolation has been extensively used worldwide for bridges. Considerable progress has been made in control methods of civil engineering structures subjected to environmental loads in the past two decades. However, in most studies, structures except isolators are assumed to be linear elastic. This paper shows the efficiency of supplementary dampers with control strategies to mitigate the large deck displacement and the hysteretic behavior of column under strong near-field ground motions. Magnetorheological dampers (MR-dampers) may be used to produce arbitral damping force vs. bridge response relations. Both external and internal damper allocations are implemented to evaluate the difference of performance.

INTRODUCTION

Seismic isolation has been extensively used worldwide for bridges. A shift of natural period as well as an increase of energy dissipation is effective to enhance the seismic performance of bridges. However deck displacement becomes excessively large when an isolated bridge is subjected to a strong near-field ground motion. Even in a standard-size bridge a deck displacement reaches 0.8m under the ground motions developed in the 1995 Kobe earthquake and 1999 Chi-Chi earthquake. It is also often the case that hysteretic deformation occurs in the plastic hinge of the columns. Such large displacements enhance the difficulty of design of expansion joints and unseating prevention devices, and large residual displacement may affect the recovery and reconstruction after earthquakes even though collapse does not occur.

This paper shows an effectiveness of supplementary dampers to mitigate the large deck displacement and the hysteretic behavior of columns. Magnetorheological dampers (MR-dampers) may be used to produce arbitral damping force vs. bridge response relations. Nonlinear seismic response of a bridge composed of low-damping isolation bearings and supplementary dampers is analyzed under five typical near-field

[1] Graduate Student, Department of Civil Engineering, Tokyo Institute of Technology, 2-12-1 O-Okayama, Meguro, Tokyo 152-8552, JAPAN, E-mail: tylee@cv.titech.ac.jp
[2] Professor, Department of Civil Engineering, Tokyo Institute of Technology, 2-12-1 O-Okayama, Meguro, Tokyo 152-8552, JAPAN, E-mail: kawasima@cv.titech.ac.jp

ground motions. Both external and internal damper allocations are implemented by numerical simulation based on optimum active control with full-state feedback to evaluate their efficiency.

In most control studies, structures except isolators are assumed to be linear elastic even under strong earthquakes. However, based on the modern bridge seismic design method, bridge columns exhibit high hysteresis to dissipate more energy. In this study, hysteretic behaviors of columns are included in the analysis as well. It was found that columns, which develop high ductility under extreme earthquakes, still exhibit hysteretic behavior and the efficiency of damping force due to classical active control method is not as remarkable as the efficiency of columns, which develop low ductility under moderate ground motions. Finally, the efficiency of isolated bridges equipped with external dampers is compared between classical optimum active control and passive control.

ISOLATED BRIDGES WITH SUPPLEMENTARY DAMPERS

Consider a nonlinear or hysteretic structure provided with supplementary energy dissipating devices and subjected to one-dimensional earthquake horizontal ground acceleration $\ddot{u}_g(t)$. The equations of motion can be described by

$$\mathbf{M}\ \ddot{\mathbf{u}}(t) + \mathbf{F}_D[\dot{\mathbf{u}}(t)] + \mathbf{F}_S[\mathbf{u}(t)] = \boldsymbol{\eta}\ \ddot{u}_g(t) + \mathbf{H}\ \mathbf{U}(t) \tag{1}$$

in which $\mathbf{u}(t), \dot{\mathbf{u}}(t), \ddot{\mathbf{u}}(t)$ are the displacement, the velocity and the acceleration vectors; $\mathbf{M}$ is the mass matrix; $\mathbf{F}_D[\dot{\mathbf{u}}(t)]$ and $\mathbf{F}_S[\mathbf{u}(t)]$ are nonlinear damping and stiffness vectors, respectively; $\mathbf{U}(t)$ is the vector of control damping forces from the supplementary dampers, and $\boldsymbol{\eta}$ and $\mathbf{H}$ are the location matrices of the excitation and control forces, respectively.

This second-order differential equation, Eq. (1) may be simplified by a transformation into the space-state form as follows:

$$\dot{\mathbf{Z}}(t) = \mathbf{g}[\mathbf{Z}(t)] + \mathbf{B}\ \mathbf{U}(t) + \mathbf{W}\ \ddot{u}_g(t) \tag{2}$$

in which $\mathbf{g}\left[\mathbf{Z(t)}\right]$ is a *2n*-vector which is a nonlinear function of the *2n*-space-state vector $\mathbf{Z}(t)$ and other matrices are defined as follows:

$$\mathbf{Z}(t) = \begin{bmatrix} \mathbf{u}(t) \\ \dot{\mathbf{u}}(t) \end{bmatrix};\ \mathbf{g}[\mathbf{Z}(t)] = \begin{bmatrix} \dot{\mathbf{u}}(t) \\ -\mathbf{M}^{-1}[\mathbf{F_D} + \mathbf{F_S}] \end{bmatrix};\ \mathbf{B} = \begin{bmatrix} 0 \\ \mathbf{M}^{-1}\mathbf{H} \end{bmatrix};\ \mathbf{W} = \begin{bmatrix} 0 \\ \mathbf{M}^{-1}\boldsymbol{\eta} \end{bmatrix} \tag{3}$$

Different control strategies can be used in order to find the control forces $\mathbf{U}(t)$ required for enhanced structural behavior.

In classical active control algorithms, the LQR performance index is given by

$$J = \int_0^{t_f} [\mathbf{Z}'(t)\mathbf{Q}\mathbf{Z}(t) + \mathbf{U}'(t)\mathbf{R}\mathbf{U}(t)]dt \tag{4}$$

in which $\mathbf{Q}$ is a $(2n \times 2n)$ symmetric positive semidefinite weighting matrix and $\mathbf{R}$ is a positive weighting matrix. In this paper, a prime indicates the transpose of either a matrix or a vector.

Referring to the generalization of optimal control theory for nonlinear structures by Yang [2], minimizing the objective function, J, given by Eq. (4) subjected to the constraint of the state equation of motion, Eq. (2) yields:

$$\mathbf{U}(t) = -0.5\mathbf{R}^{-1}\mathbf{BPZ}(t) \tag{5}$$

$$\mathbf{\Lambda_0}'\mathbf{P} + \mathbf{P}\mathbf{\Lambda_0} - 0.5\mathbf{PBR}^{-1}\mathbf{B}'\mathbf{PZ}(t) = -2\mathbf{Q} \tag{6}$$

in which $\mathbf{P}$ is the Riccati matrix where

$$\mathbf{\Lambda_0} = \partial\mathbf{g}(\mathbf{Z})/\partial\mathbf{Z}|_{\mathbf{Z}=0} \tag{7}$$

Note that Eq. (6) is approximated by neglecting the earthquake ground acceleration $\ddot{u}_g(t)$ and by linearizing the structural system at the initial equilibrium point $Z = 0$. Since the term $\mathbf{PBR}^{-1}\mathbf{B}'\mathbf{P}$ is positive semidefinite, Eq. (7) can be approximated further by

$$\mathbf{\Lambda_0}'\mathbf{P} + \mathbf{P}\mathbf{\Lambda_0} = -2\mathbf{Q} \tag{8}$$

which is known as the Lyapunov equation.

One can also prescribe the control forces to be passive damping forces, such as viscous damper or spring damper. The forces from the passive dampers can be expressed as

$$\mathbf{U}(t) = [U_1(t), U_2(t), \ldots, U_n(t)]' \tag{9}$$

$$U_i(t) = -k_{di}x_i(t) - c_{di}\dot{x}(t) \quad \text{for } i = 1,2,\ldots,n \tag{10}$$

in which k_{di} and c_{di} are the equivalent linear elastic stiffness and viscous damping coefficients, respectively, x_i is the stroke of the passive damper.

The bridge structure and isolated bearing may be idealized to be nonlinear or hysteretic. The following hysteretic model is used for both the bridge structure and isolator. The stiffness restoring force is given by Bouc-Wen model.

$$F_{si}(t) = \alpha_i k_i x_i(t) + (1-\alpha_i)k_i x_{yi} v_i \tag{10}$$

in which x_i = deformation of the ith element, k_i = elastic stiffness, α_i = ratio of the post-yielding to pre-yielding stiffness, x_{yi} = yielding deformation, and v_i = hysteretic variable with $|v_i| \le 1$, where

$$\dot{v}_i = x_{yi}^{-1}\left[A_i\dot{x}_i - \beta_i|\dot{x}_i||v_i|^{n_i-1}v_i - \gamma_i\dot{x}|v|^{n_i}\right] \tag{11}$$

in which parameters A_i, β_i, γ_i and n_i govern the scale, general shape and smoothness of the hysteresis loop. Note that the ith element is linear elastic if $\alpha_i = 1$.

SEISMIC RESPONSES OF ISOLATED BRIDGES

A target bridge with isolators is considered as shown in Fig. 1. MR dampers may be installed between the deck and the column or the deck and the abutment. When MR dampers are connected to the abutment, they are regarded as applying external force to the bridge. On the other hand, when MR dampers are connected to the deck, the damping forces are regarded as part of internal forces. The effectiveness of both allocations will be discussed respectively. Assuming that the soil is stiff, the response of bridge may be idealized as a two degree of freedom system as shown in Fig. 2. The mass of deck and column are 700T and 140T, respectively. The columns exhibit bilinear elastoplastic behavior with zero post-yield stiffness, whereas the isolator is elastomeric with low damping, Fig. 3. The fundamental natural period of the entire bridge is 1.3 second. For simplicity, the damping of the system is assumed as linear viscous and the damping ratio is 2% for the two modes.

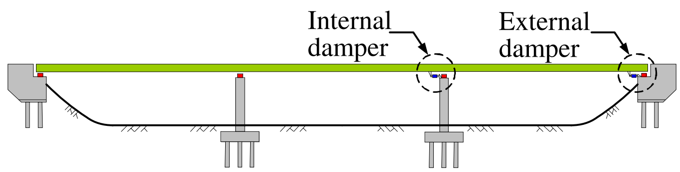

Figure 1 Target Bridge

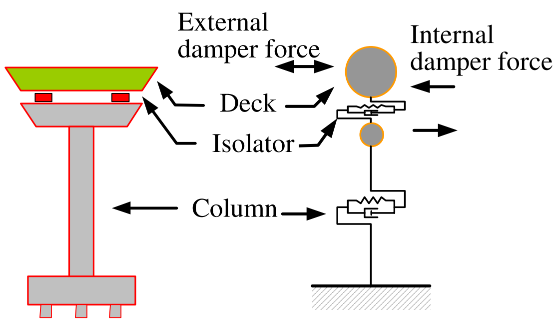

Figure 2 Analytical Idealization

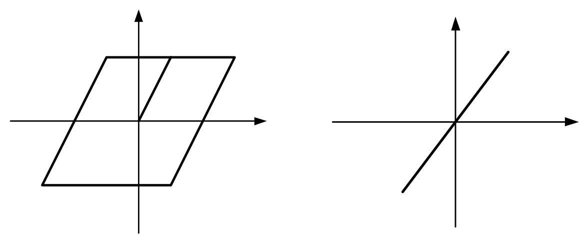

Figure 3 Material Behavior of Column and Isolator

Used are JMA Kobe Observatory and JR-Takatori Station in the 1995 Kobe, Japan earthquake, Duzce in the 1999 Duzce, Turkey earthquake, Sylmar Parking Lot in the 1994 Northridge, USA earthquake, and Sun-Moon Lake in 1999 Chi-Chi, Taiwan earthquake, as shown in Fig. 4. All the excitations are applied at the full intensity for the evaluation of the performance indices.

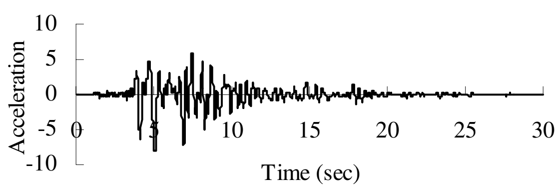

(a) JMA Kobe Observatory

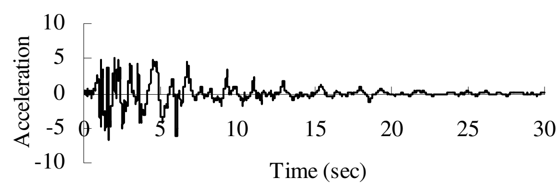

(b) JR-Takatori Station

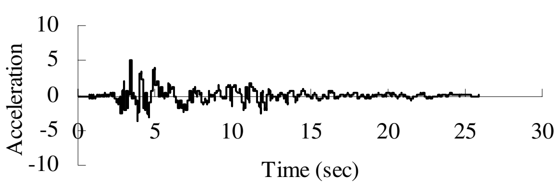

(c) Duzce

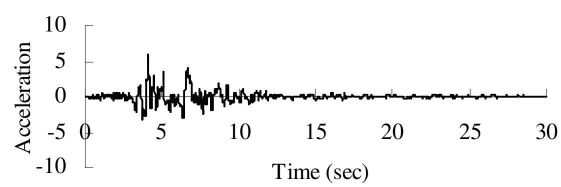

(d) Sylmar Parking Lot

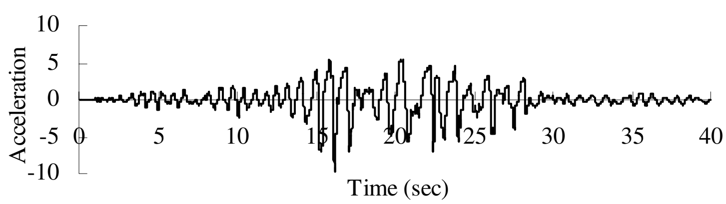

(e) Sun-Moon Lake

Figure 4 Ground Motions (m/sec^2)

With the MR damper applying the control force to the bridge, the structural response depends on the weighting matrices $\mathbf{Q}$ and $\mathbf{R}$. For this example, the $\mathbf{Q}$ matrix is considered as a diagonal matrix with all the diagonal elements equal to one. Since the $\mathbf{R}$ weighting matrix consists of only one element and the magnitude of required control damping force mainly depends on $\mathbf{R}$ value, $\mathbf{R}$ value is implemented over a wide range in order to evaluate and search for the suitable $\mathbf{R}$ value under the feasible capacity of devices. In some studies, considering that the required control force may be too large when the earthquake excitation is strong, saturated controller is adopted to bound the control force. In this study, control force will not be limited but only control force below 40% of deck weight is evaluated.

Time histories of all the response quantities are computed within 30 seconds of the records except Chi-Chi earthquake with 40 seconds. The generated control damping force, and the corresponding displacement and absolute acceleration of deck and column are evaluated using normalized indices. Generated control damping force is normalized by the deck weight. Displacement and absolute acceleration are normalized by the corresponding magnitudes in the uncontrolled structure. The results of the evaluations for external damper and internal damper are presented as follows.

External damper

Time history displacement responses for JMA Kobe and Sun-Moon Lake earthquakes with $\mathbf{R}$ of 5×10^{-12} are shown in Figs. 5 and 6. The hysteretic loops of the column and isolator are also shown in Figs. 7 and 8. The corresponding stroke and damping force hystereses of the MR damper are shown in Fig. 9. As observed from the results, displacement responses are reduced from the uncontrolled responses. The column even exhibits elastic response using controlled damper under JMA Kobe record, while column displacement ductility factor decreases from 11.8 to 6.9 under Sun-Moon Lake record.

The performance indices described above with respect to weighting $\mathbf{R}$ for five ground motions are shown in Fig. 10. The column displacement ductility factor without control is 4.1, 3.8 and 1.1 under JMA Kobe, Duzce and Sylmar records, respectively, while it is 9.2 and 11.8 under JR-Takatori and Sun-Moon Lake records, respectively, which are not shown in Fig. 10(d). The higher ductility factor in uncontrolled bridge, the higher control damping force is generated as shown in Fig. 10(a). However, even though higher control force is applied, the deck displacement under Sun-Moon Lake and JR-Takatori do not reduce to the level developed under other records except Sylmar, as shown in Figs. 10(b), and it is important to note that column still exhibits high inelastic behavior as shown in Fig. 10(d). One can attribute it to the insufficient assumption in the linearization of the bridge that the initial stiffness is used to determine the gain vector of control force for both linear and nonlinear ranges.

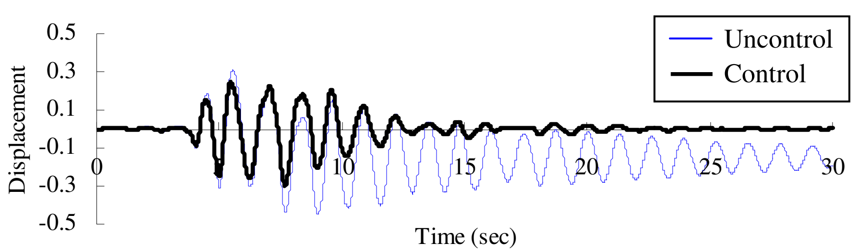

(a) Deck Displacement (m)

Figure 5 Displacements Responses under JMA Kobe

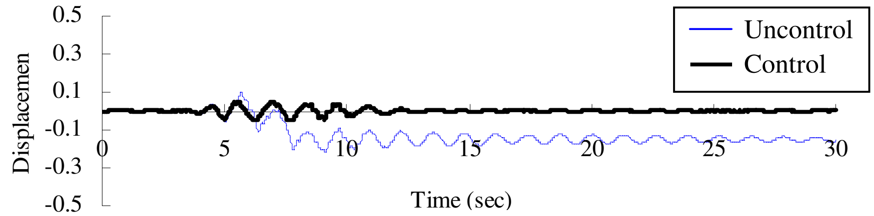

(b) Column Displacement (m)

Figure 5-conti. Displacements Responses under JMA Kobe

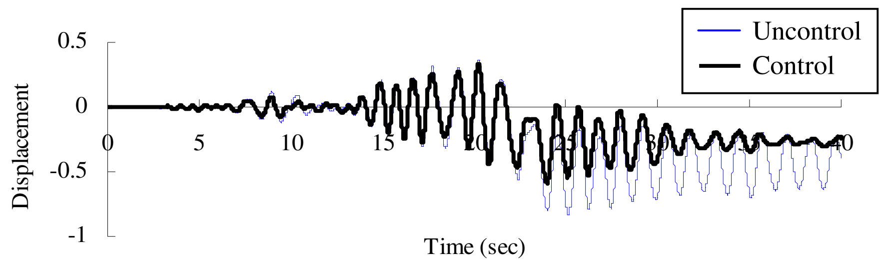

(a) Deck Displacement (m)

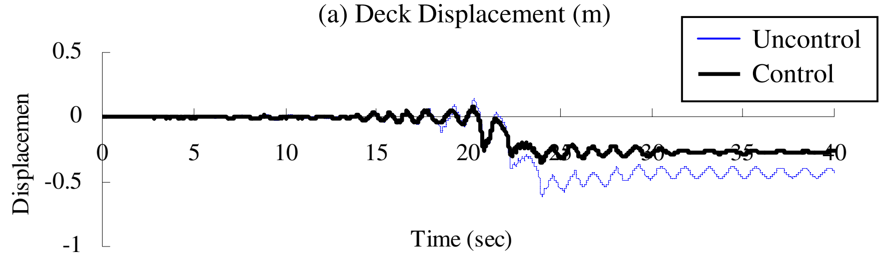

(b) Column Displacement (m)

Figure 6 Displacements Responses under Sun-Moon Lake

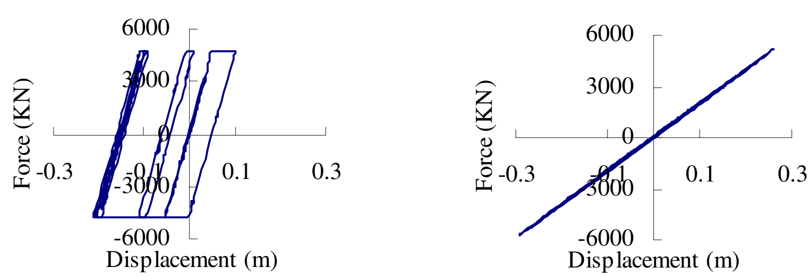

Column **Isolator**

(a) Uncontrol

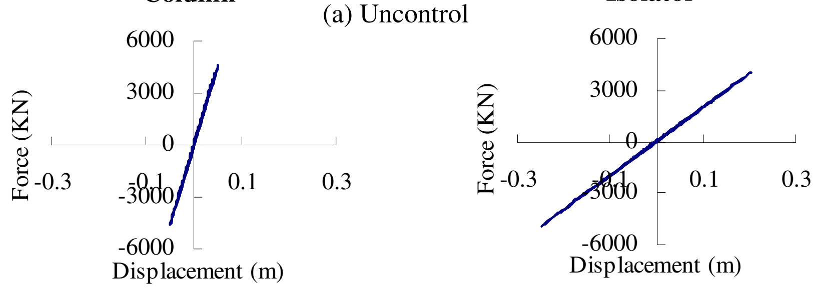

Column **Isolator**

(b) Control

Figure 7 Hysteretic Loops under JMA Kobe

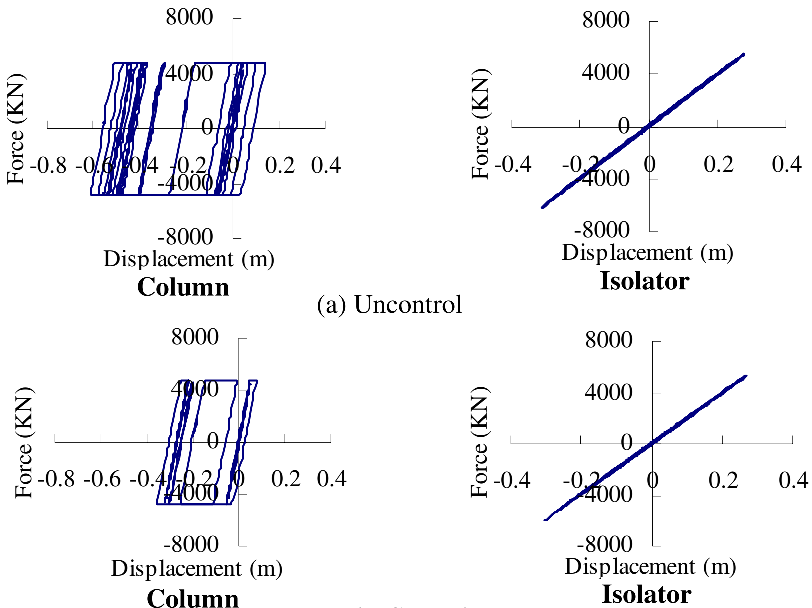

(a) Uncontrol

(b) Control

Figure 8 Hysteretic Loops under Sun-Moon Lake

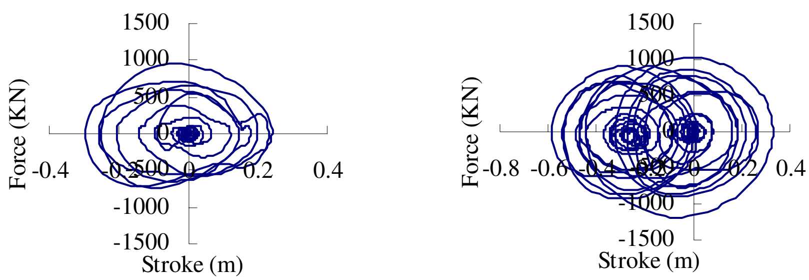

(a) JMA Kobe (b) Sun-Moon Lake

Figure 9 Damping Force v.s. Stroke Hystereses

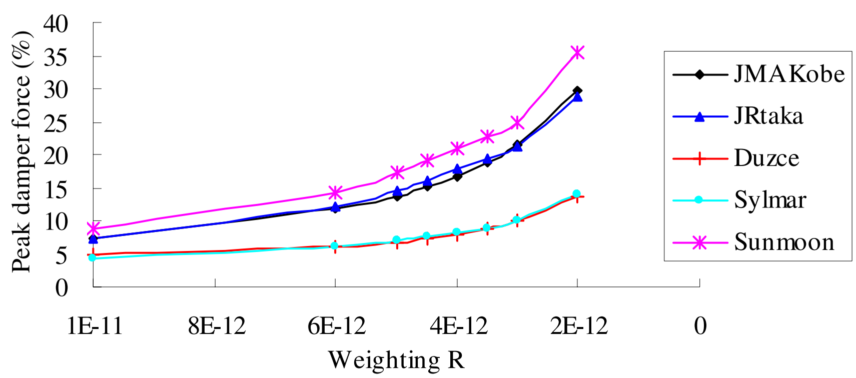

(a) Normalized peak damper force

Figure 10 Performance Indices v.s. Weighting R of External Dampers under Five Excitations

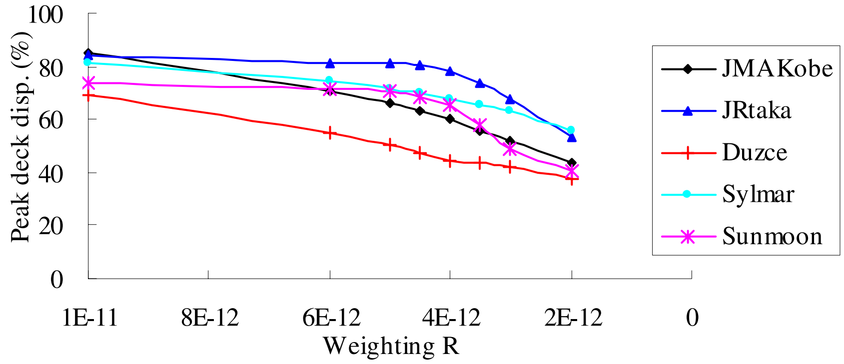

(b) Normalized peak deck displacement

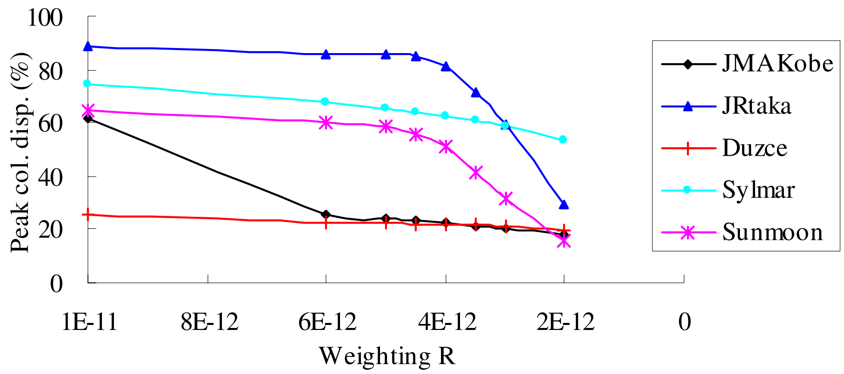

(c) Normalized peak column displacement

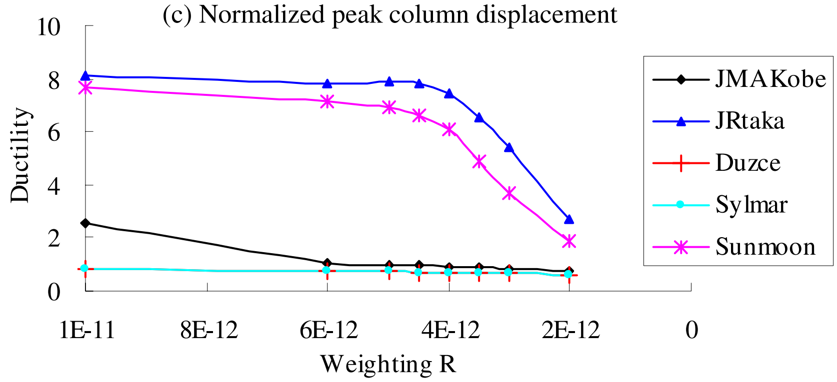

(d) Column ductility

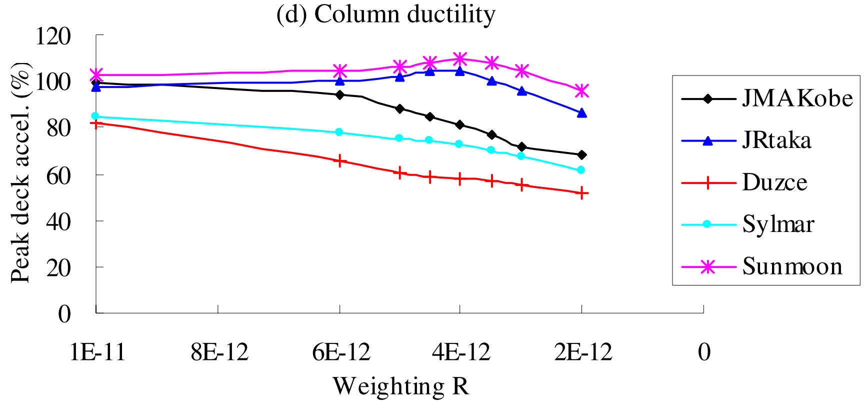

(e) Normalized peak deck acceleration

Figure 10-conti. Performance Indices v.s. Weighting R of External Dampers under Five Excitations

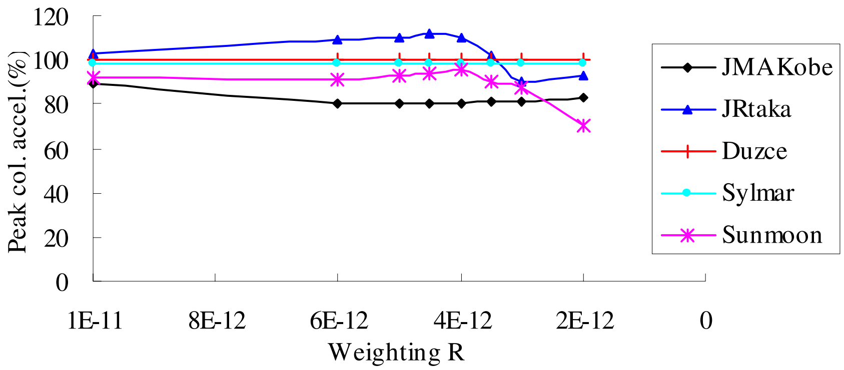

(f) Normalized peak column acceleration

Figure 10-conti. Performance Indices v.s. Weighting R of External Dampers under Five Excitations

Internal damper

Time history displacement responses of the deck and the column under JMA Kobe and Sun-Moon Lake records with **R** of 5×10^{-12} are shown in Figs. 11 and 12. The hysteretic loops of the column and isolator are also shown in Figs. 13 and 14. The corresponding stroke and damping force hystereses of the MR damper are shown in Fig. 15. Using the controlled damper, both the deck and column displacements can be decreased, but still some inelastic deformation occurs in the column.

The performance indices with respect to weighting **R** for five ground motions are shown in Fig. 16. As same as the external damper, the deck displacement under Sun-Moon Lake and JR-Takatori do not reduce to the level developed under other records as shown in Figs. 16(b) even though higher control force is applied as shown in Fig. 16(a). One can also attribute it to the insufficient assumption in the linearization of the bridge that the initial stiffness is used to determine the gain vector of control force for both linear and nonlinear ranges. Note that column still exhibits hysteretic behavior compared to the same level of control force applied by the external damper under all ground motions except Sylmar as shown in Fig. 16(d). In addition, the decrease of deck and column displacements results in an increase of deck accelerations because the internal damping force restricts the relative displacement between the deck and the column as shown in Fig. 16(e).

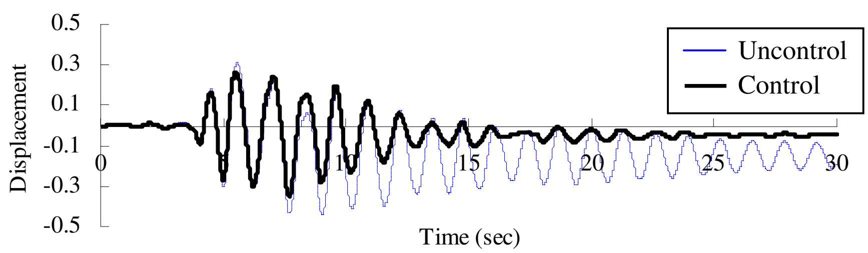

(a) Deck Displacement (m)

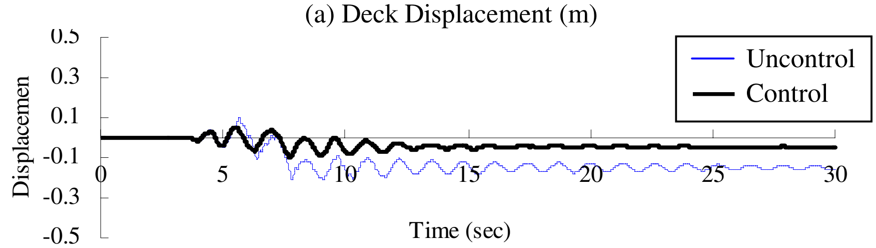

(b) Column Displacement (m)

Figure 11 Displacements Responses under JMA Kobe

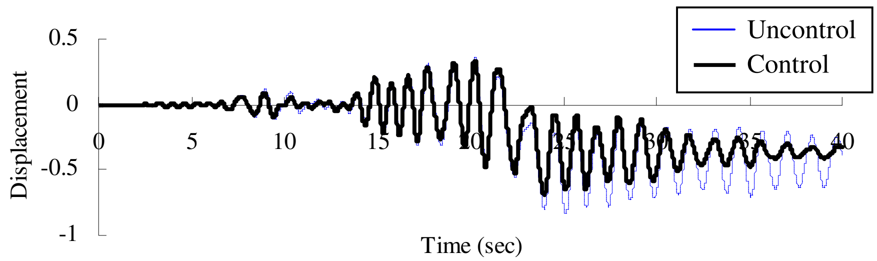

(a) Deck Displacement (m)

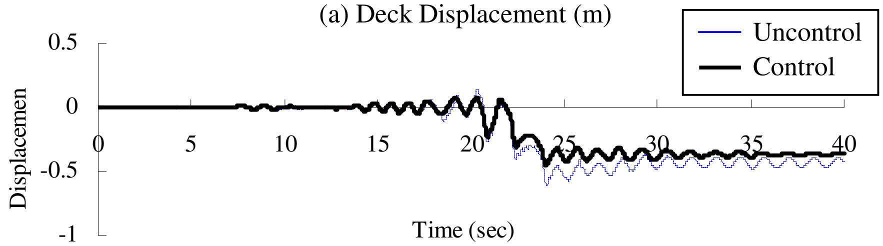

(b) Column Displacement (m)

Figure 12 Displacements Responses under Sun-Moon Lake

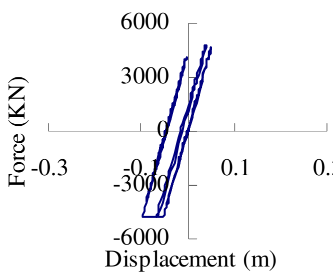

Column

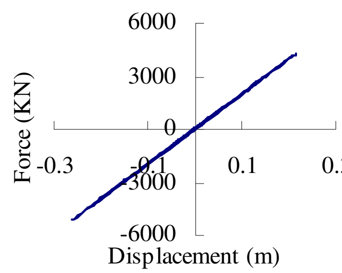

Isolator

Figure 13 Hysteretic Loops under JMA Kobe

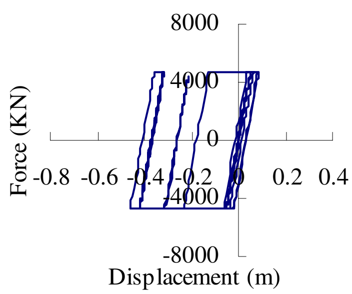

Column

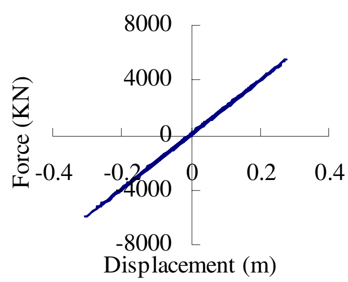

Isolator

Figure 14 Hysteretic Loops under Sun-Moon Lake

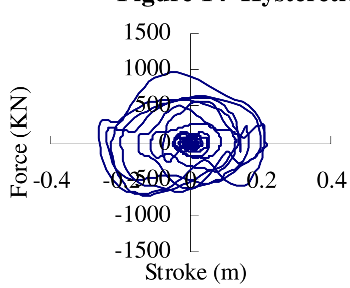

(a) JMA Kobe

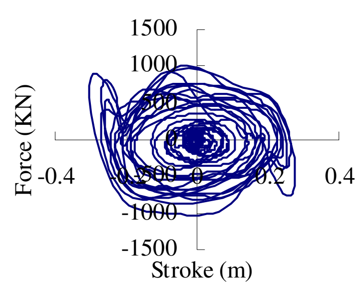

(b) Sun-Moon Lake

Figure 15 Damping Force v.s. Stroke Hystereses

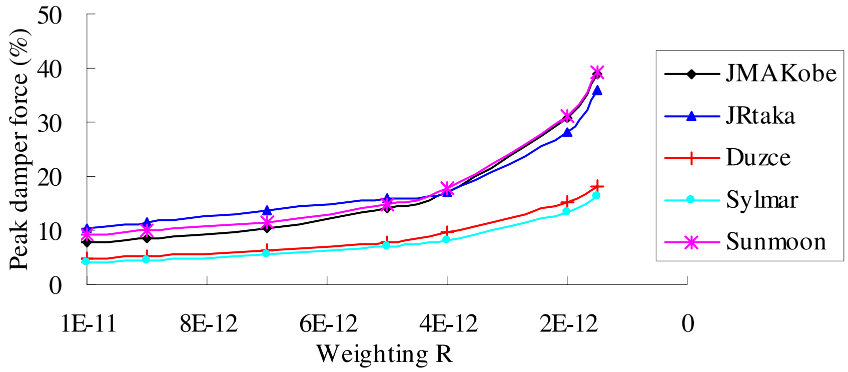

(a) Normalized peak damper force

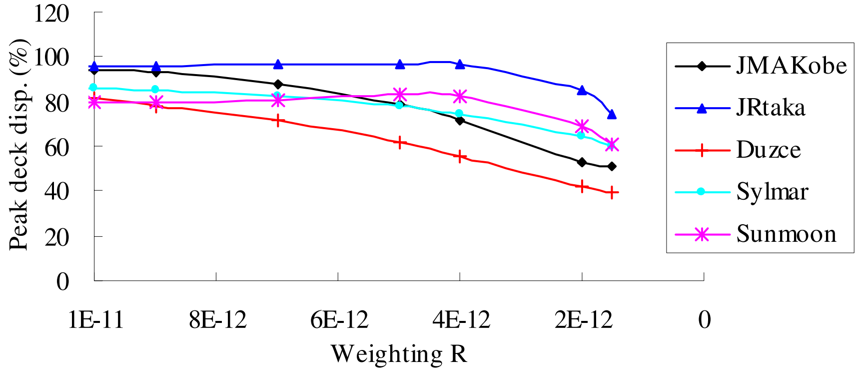

(b) Normalized peak deck displacement

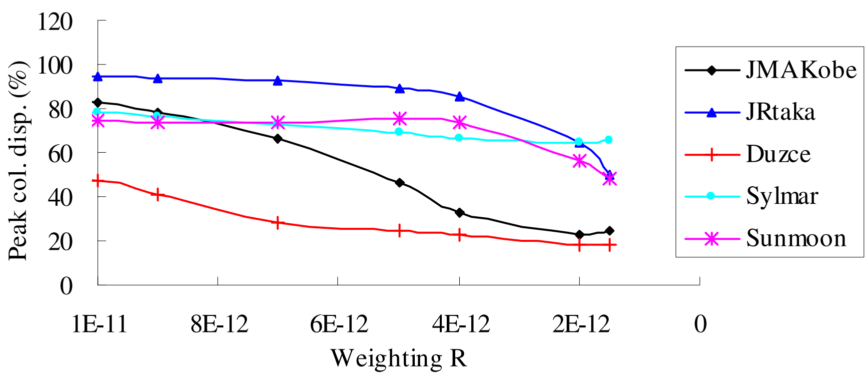

(c) Normalized peak column displacement

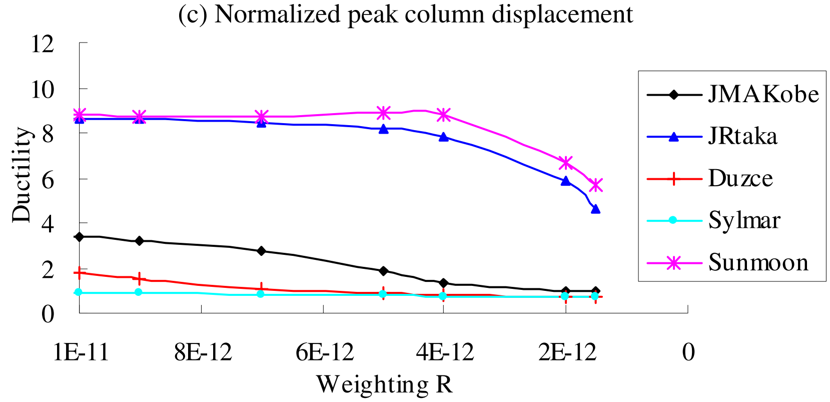

(d) Column ductility

Figure 16 Performance Indices v.s. Weighting R of External Dampers under Five Excitations

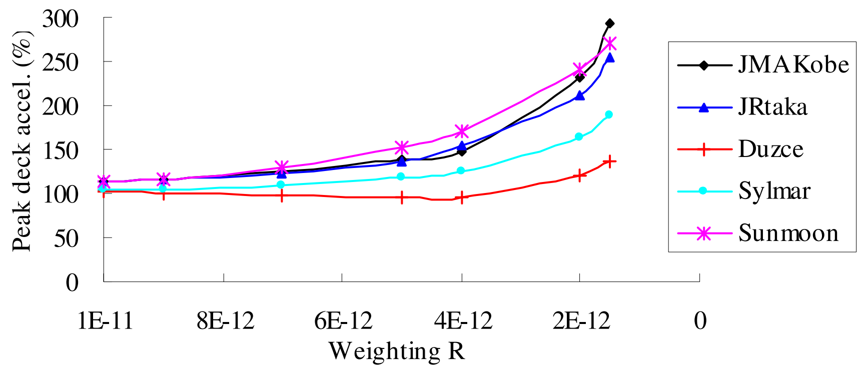

(e) Normalized peak deck acceleration

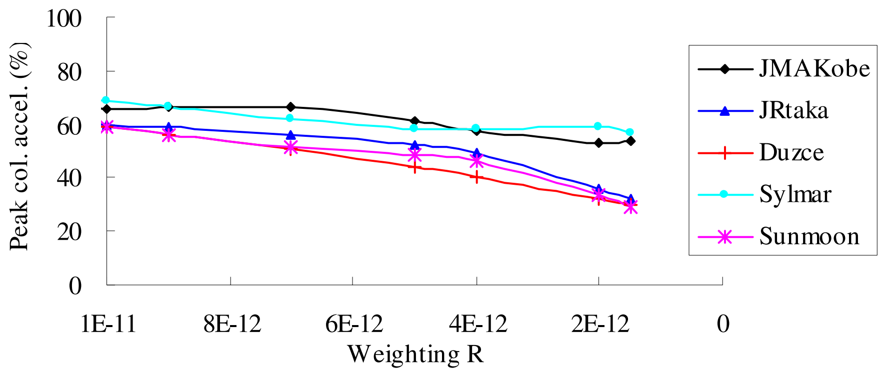

(f) Normalized peak column acceleration

Figure 16-conti. Performance Indices v.s. Weighting R of External Dampers under Five Excitations

COMPARISON OF CLASSICAL OPTIMUM ACTIVE CONTROL AND PASSIVE CONTROL

In order to compare the efficiency of the classical optimum active control and passive control on structures with nonlinear behavior under extreme earthquakes, the passive control with viscous damper are used. Used are JMA Kobe Observatory and JR-Takatori Station in the 1995 Kobe, Japan earthquake, and Sun-Moon Lake in 1999 Chi-Chi, Taiwan, earthquake, which develop higher inelastic behavior on columns as shown above. All the excitations are applied at the full intensity for the evaluation of the performance indices. Time histories of all the response quantities are the same as above. The generated control damping force, and the corresponding displacement and absolute acceleration of deck and column are evaluated using normalized indices as well. Since the external damper shows higher efficacy than the internal damper and no penalty of increasing deck acceleration, the comparison will be focused on the external dampers.

The $\mathbf{R}$ value is implemented from 2×10^{-12} to 1×10^{-11} in the optimum active control with $\mathbf{Q}$ matrix is considered as a unit diagonal matrix while the viscous damping coefficient c_{di} is implemented from 200 KN-sec/m to 4000 KN-sec/m with $k_{di}=0$ in the passive control. The performance indices with respect to the maximum damping force generated under the three ground motions are shown in Fig. 17. It is interesting that the performance indices of both active and passive control strategies almost coincide with each other. As a matter of fact, the gain vector $\mathbf{U}(t)$ in Eq. (5) of active control algorithm can be rewritten as

$$\mathbf{U}(t) = \mathbf{G}_1\mathbf{u}(t) + \mathbf{G}_2\dot{\mathbf{u}}(t) = -\mathbf{K}_a\mathbf{x}(t) - \mathbf{C}_a\dot{\mathbf{x}}(t) \tag{12}$$

The term $\mathbf{C_a}\dot{\mathbf{x}}(t)$ dominates the active control force, and the coefficients of $\mathbf{C_a}$ corresponding to c_{di} in Eq. (10) are almost identical and the other coefficients are insignificant.

The column exhibits high displacement ductility factor in the uncontrolled bridge under Sun-Moon Lake and JR-Takatori records. It is important to note that column still exhibits high inelastic behavior as shown in Fig. 17(c) even though the normalized generated control force reaches 30%. The deck displacement does not reduce to the level, which can be realized by 10%-30% normalized damping force under JMA Kobe record, as shown in Figs. 17(a). However, as the higher maximum damping force increases, the peak deck displacement and column displacement ductility decreases are reduced generally.

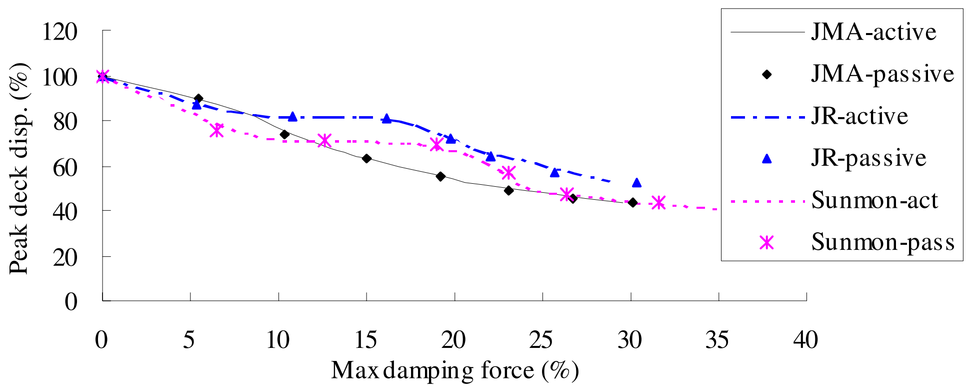

(a) Normalized peak deck displacement

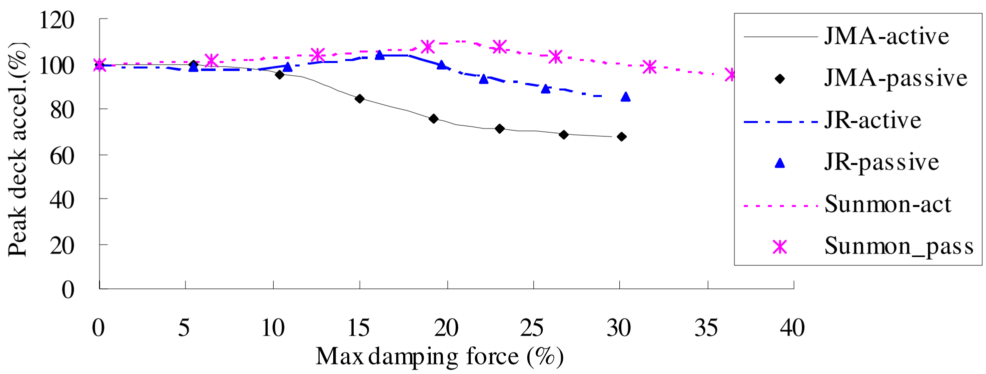

(b) Normalized peak deck acceleration

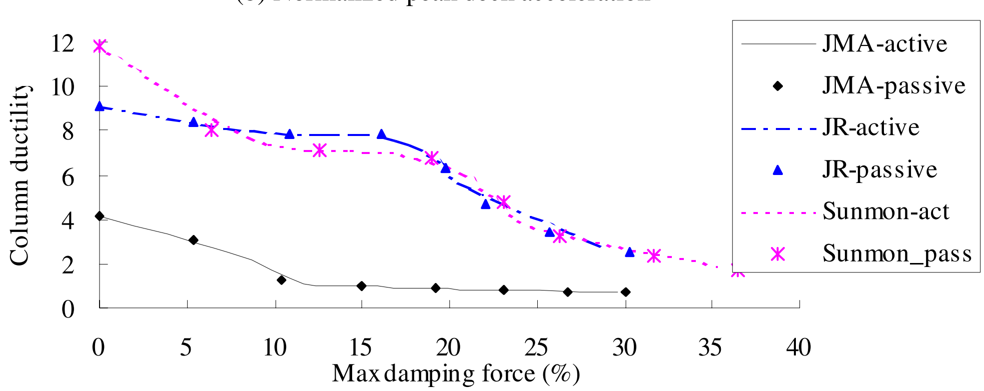

(c) Column ductility

Figure 17 Performance Indices v.s. Maximum Damping Force

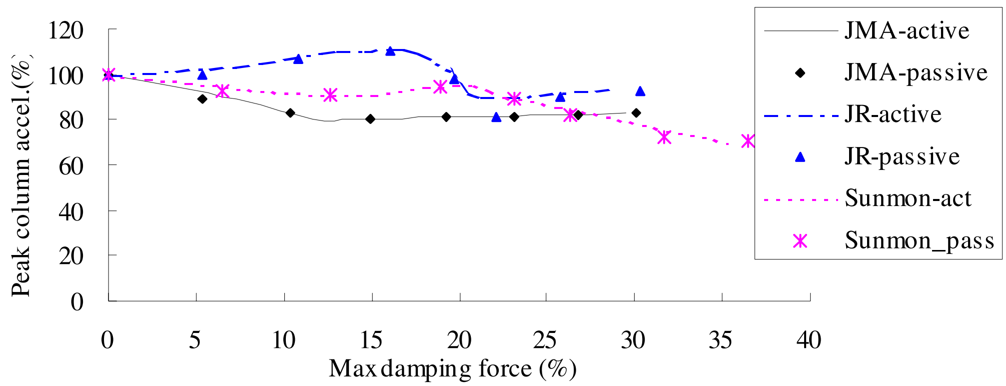

(d) Normalized peak column acceleration

Figure 17-conti. Performance Indices v.s. Maximum Damping Force

CONCLUSIONS

The feasibility and effectiveness of supplementary dampers for controlling the seismic response of isolated bridges were evaluated based on numerical simulations under five near-field ground motions. The damper allocations investigated include the external damper and the internal damper. The following conclusions may be obtained from the results presented herein.

1. Both damper allocations are effective for active control in reducing the deck displacement subjected to the near-field ground motions. Especially, the external damper shows higher efficacy than the internal damper and no penalty of increasing deck acceleration. However the external damper may only be installed at the ends of bridges such as abutments. It is limited for wider application in seismic design.
2. The magnitude of damper force required for control depends on not only the weighting $\mathbf{R}$ but also the intensity and characteristic of ground excitation. In addition, the performance indices extensively vary depending on ground motions so that one should pay an attention on the type of ground motions to maintain the stability of control.
3. Under the control using a feasible level of damping force, the effectiveness of supplementary dampers reduces as the plastic deformation of the column becomes significant. Further improvement of the control method that can be applied to bridges with high nonlinearity is required.
4. No matter how the supplementary dampers are controlled by the classical optimum active control with full-state feedback, its effectiveness is nearly the same with the viscous damper.

REFERENCES

1. Kawashima, K. and Unjoh, S. "Seismic Response Control of Bridges by Variable dampers," Journal of Structural Engineering, ASCE 1994, 120(9), 2583-2601.
2. Yang, J.N., Li, Z. and Vongchavallitkul, S. "A Generalization of Optimal Control Theory: Linear and Nonlinear Control," Journal of Engineering Mechanics, ASCE 1994, 120(2), 266-283.
3. Yang, J.N., Wu, J.C., Kawashima, K. and Unjoh, S. "Hyrid Control of Seismic-excited Bridge Structures," Earthquake Engineering and Structural Dynamics 1995, 24(11), 1437-1451.